Water Resources Research

RESEARCH ARTICLE
10.1029/2018WR024029

Harmonic Pulse Testing for Well Monitoring: Application to a Fractured Geothermal Reservoir

E. Salina Borello[1], P. A. Fokker[2,1], D. Viberti[1], F. Verga[1], H. Hofmann[3], P. Meier[4], K.-B. Min[5], K. Yoon[6], and G. Zimmermann[3]

[1]Politecnico di Torino, Turin, Italy, [2]TNO Applied Geosciences, Utrecht, The Netherlands, [3]GFZ - German Research Centre for Geosciences, Potsdam, Germany, [4]Geo-Energie Suisse AG, Zürich, Switzerland, [5]Department of Energy Resources Engineering, Seoul National University, Seoul, South Korea, [6]Nexgeo, Seoul, South Korea

Key Points:
- An advanced methodology for well performance monitoring without production interruption is presented
- Diagnostic plots analogous to oil industry conventional well testing for flow geometry and regime identification were adopted
- A field case validation shows the successful application of the methodology to monitor the stimulation of a well of an enhanced geothermal system

Supporting Information:
- Supporting Information S1

Correspondence to:
E. Salina Borello,
eloisa.salinaborello@polito.it

Citation:
Salina Borello, E., Fokker, P. A., Viberti, D., Verga, F., Hofmann, H., Meier, P., et al. (2019). Harmonic pulse testing for well monitoring: Application to a fractured geothermal reservoir. *Water Resources Research*, *55*. https://doi.org/10.1029/2018WR024029

Received 11 SEP 2018
Accepted 27 APR 2019
Accepted article online 6 MAY 2019

Abstract Harmonic Pulse Testing (HPT) has been developed as a type of well testing applicable during ongoing field operations because a pulsed signal is superimposed on background pressure trend. Its purpose is to determine well and formation parameters such as wellbore storage, skin, permeability, and boundaries within the investigated volume. Compared to conventional well testing, HPT requires more time to investigate the same reservoir volume. The advantage is that it does not require the interruption of well and reservoir injection/production before and/or during the test because it allows the extraction of an interpretable periodic signal from measured pressure potentially affected by interference. This makes it an ideal monitoring tool. Interpretation is streamlined through diagnostic plots mimicking conventional well test interpretation methods. To this end, analytical solutions in the frequency domain are available. The methodology was applied to monitor stimulation operations performed at an Enhanced Geothermal System site in Pohang, Korea. The activities were divided into two steps: first, a preliminary sequence of tests, injection/fall-off, and two HPTs, characterized by low injection rates and dedicated to estimate permeability prior to stimulation operations, and then stimulation sequence characterized by a higher injection rate. During the stimulation operations other HPT were performed to monitor formation properties behavior. The interpretation of HPT data through the derivative approach implemented in the frequency domain provided reliable results in agreement with the injection test. Moreover, it provided an estimation of hydraulic properties without cessation of stimulation operations, thus confirming the effectiveness of HPT application for monitoring purposes.

1. Introduction

Knowledge of hydraulic parameters is essential for the understanding and quality management of geothermal operations. The standard way of obtaining hydraulic parameters is well testing. However, conventional well testing cannot be employed as a monitoring tool during stimulation and it is challenging to employ during ongoing production or injection operations because it requires preliminary well shut-in. Therefore, Harmonic Pulse Testing (HPT) has been used as a well testing methodology for estimating the hydraulic properties of a formation without stopping production or injection operations (Fokker et al., 2018).

HPT, in a similar way to Periodic Hydraulic Testing, is characterized by a periodic variation of injection or production rates. The concept was first proposed by Kuo (1972) and has since been developed for the determination of hydraulic parameters by several authors (Black & Kipp, 1981; Cardiff & Barrash, 2015; Despax et al., 2004; Hollaender, Hammond, & Gringarten, 2002), in different scenarios like biphase flow (Fokker & Verga, 2011), fractured well (Morozov, 2013; Vinci et al., 2015), fractured reservoir (Guiltinan & Becker, 2015), gas well (Salina Borello et al., 2017), and horizontal well (Fokker et al., 2018). It was also suggested for the characterization of heterogeneous reservoir (Ahn & Horne, 2010; Cardiff et al., 2013; Copty & Findikakis, 2004; Fokker et al., 2012; Rosa & Horne, 1997), fault hydraulic properties (Chen & Renner, 2018), and leakage from faults (Sun et al., 2015). Some real applications of HPT are documented in the literature for a field of three wells penetrating a heterogeneous aquifer (Fokker et al., 2013; Renner & Messar, 2006); single and multilayer reservoirs (Rochon et al., 2008); a gas storage field confined by a lateral aquifer (Salina Borello et al., 2017); and a horizontal well in a gas storage field (Fokker et al., 2018).

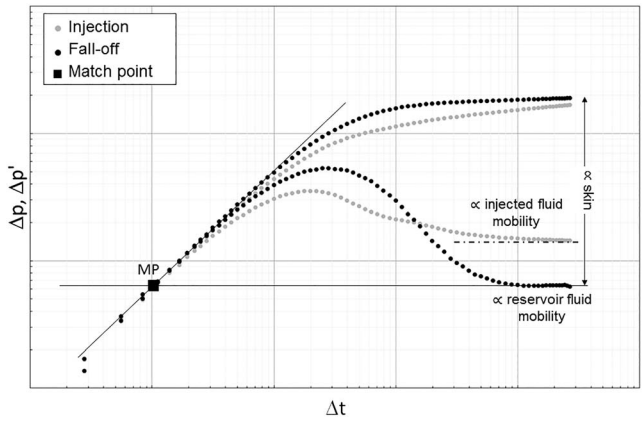

Figure 1. Schematic of injection/fall-off test log-log plot.

The goals of HPT are similar to those of conventional well testing: the assessment of well and reservoir properties such as well damage (skin), wellbore storage (C), formation permeability (k), and presence of boundaries in the investigated area. However, the interpretation of the pressure development is performed in the frequency domain. Pressure response to the imposed periodic rate changes is isolated from other effects like interference due to production/injection operations from neighboring wells through the identification of discrete frequencies. The main drawback of HPT is that it requires more time than conventional testing to obtain the same information (Hollaender, Hammond, & Gringarten, 2002). For this reason, it may be unsuitable when the volume of interrogation required is large, as in the case of reservoir boundary assessment from exploration and appraisal wells, but it is appropriate for monitoring well performance during ongoing operations.

Fokker et al. (2018) presented a more general approach by following the practice of type curve matching developed in conventional well testing and allowing a more straightforward determination of permeability, skin, wellbore storage, and reservoir boundary characteristics. In the present contribution, we target the validation of the technology as a monitoring tool during a real stimulation treatment. We used the stimulation operation performed at the Enhanced Geothermal System (EGS) site in Pohang, Korea, in August 2017 in well PX-1. The injection operations sequence was designed to characterize the formation permeability before the stimulation operations and to monitor the evolution of formation permeability during the stimulation.

To this end, a preliminary injection/fall-off test and two harmonic pulse tests (HPT-1 and HPT-2) characterized by low rates were performed as a baseline for permeability estimation before the actual stimulation operations, which were characterized by higher rates. Subsequently, nine harmonic pulse tests were performed during the stimulation on top of a background injection rate. This makes the test an ideal candidate for demonstrating the utility of HPT as a monitoring tool.

2. Injection Testing and HPT

A brief introduction to injection tests and harmonic pulse tests is provided in this section; a detailed description of the interpretative models for harmonic testing is given in Appendix A.

2.1. Injection Test: Principles and Interpretation

An injection test is aimed at assessing reservoir characteristics and well performance. It has gained attention over the last 20 years in the oil and gas industry (El-Khazindar et al., 2002; Hollaender, Filas et al., 2002; Verga & Rocca, 2010; Rocca & Viberti, 2013; Verga & Rocca, 2010; Verga & Salina Borello 2016; Woie et al., 2000). Some authors have dedicated to the study and development of interpretation methodologies based on analytical models (Banerjee et al., 1998; Barreto et al., 2011; Boughrara et al., 2007; Habte & Onur, 2014; Levitan, 2003), numerical models (Verga et al., 2008, 2014), or hybrid interpretation approaches that adopt numerical simulation along with standard monophasic models (Verga et al., 2011, 2012). Successful real cases have also been documented (Azzarone et al., 2011; Beretta et al., 2007; Tripaldi et al., 2009).

One reason for the increased popularity of injection testing is its operational simplicity and the minimal environmental impact: no produced fluids need to be disposed of.

In oil field applications an injection test consists of injecting fluid, commonly brine or diesel, in a potential oil pay zone and in monitoring the pressure response during the injection period and the subsequent fall-off period, in which the well is shut in and the pressure tends to return to the equilibrium value. The derivative of pressure variation of the fall-off period with respect to the natural logarithm of time increment is plotted on a log-log scale against the time increment to identify flow geometries and flow regimes (Bourdet, 2002). A schematic log-log plot is provided in Figure 1, where ∝ is the proportionality symbol. The intersection between lines identifying wellbore storage (slope 1) and radial flow (horizontal stabilization, slope 0) is called match point (MP), whose coordinates (x_{MP}, y_{MP}) allow to estimate wellbore storage and reservoir

permeability, respectively. In particular, permeability value is obtained under the assumption of constant net producing thickness and fluid viscosity. Moreover, derivative matching via analytical type curves for single-phase flow (Bourdet et al., 1983; Gringarten et al., 1979) allows the identification of well productivity through skin factor, possibly corrected for two-phase interaction (Beretta et al., 2007).

In the case of injection of water into an aquifer, the injected fluid and the fluid in place are miscible; consequently, relative permeabilities do not play a role. However, a difference in temperature may exist between reservoir water and injected water. Therefore, even if the effective permeability is the same during the injection and the fall-off period, the infinite acting radial flow (IARF) horizontal stabilization exhibited by the derivative of the two flow periods could be significantly different (Levitan, 2003) because of the variation in fluid viscosity. From the fall-off period derivative analysis the following reservoir properties can be derived:

1. Reservoir permeability (k) is determined from the horizontal stabilization (y_{MP}) (Bourdet, 2002):

$$k = \frac{qB\mu}{4\pi h}\frac{1}{y_{MP}} \tag{1}$$

The obtained permeability (k) is an average value over the radius of investigation of the test (r_i), which is proportional to the fall-off duration (Δt_{fo}) (Lee, 1982):

$$r_i = 1.5\sqrt{\frac{k\Delta t_{fo}}{\mu c_t \phi}} \tag{2}$$

Notice that the investigation radius is independent from the flow rate (q) while it is directly dependent on permeability (k). A complete list of symbols is reported at the end of the paper in the Nomenclature section.

2. Wellbore storage (C), accounting for the compression of injected fluid stored in the wellbore is determined by the intersection x_{MP} of horizontal stabilization and the wellbore storage line of slope one as (Bourdet, 2002)

$$C = \frac{2kh}{\mu}x_{MP} \tag{3}$$

3. Skin (S), expressing the flow restriction/improvement due to well damage/stimulation, is related to the distance between stabilization of the derivative and pressure increment and is identified via type curve matching. Skin value may be influenced by the near-wellbore volume of cumulatively injected water, which is characterized by a lower mobility due to higher viscosity.

A great advantage of the derivative approach is that it allows decoupling the effect on pressure response of near-wellbore transmissibility from wellbore storage and skin.

The analysis is further supported by the reconstruction of pressure profile and Horner plot (Horner, 1951), a semilog plot in which pressure is plotted against the so-called superposition time:

$$\text{superposition time} = \frac{t_p + \Delta t}{\Delta t} \tag{4}$$

where t_p is the duration of the injection period, and Δt is the time elapsed from shut-in.

2.2. Harmonic Pulse Testing

In principle, a harmonic well test employs a sinusoidal signal on the flow rate and records the resulting pressure response. This response does not only show a magnitude but also a phase shift, which is the delay of the pressure oscillation with respect to the imposed flow oscillation. The amplitude ratio between imposed rate and pressure response, and the phase shift between them depend on reservoir and well properties in the volume of investigation, such as fluid mobility, total compressibility, skin, and wellbore storage. Interpretation of the response thus allows characterizing the system.

Table 1
Reservoir and Well Parameters Adopted as Input Data for Interpretation

Water viscosity (μ_w)	0.22 mPa s
Total compressibility (c_t)	$4.86 \cdot 10^{-10}$ Pa^{-1}
Porosity (ϕ)	0.01
Well radius (r_w)	0.10795 m

Under standard well operation procedures it is much easier to generate rectangular pulses with alternating periods of fixed rates than sinusoidal signals. Rectangular pulses can be decomposed into an array of harmonic components with distinct frequencies, using Fourier transformation. A single test performed using rectangular rate pulses then corresponds to the simultaneous execution of a number of tests each representing a single harmonic component. As a consequence a rectangular rate pulse test contains more information than a sinusoidal harmonic test, which is characterized by a single component. Pulses with oscillation period T_f (duration $T_f/2$ with a high rate and $T_f/2$ with a low rate) contain harmonic components with oscillation periods T_f, $T_f/3$, and $T_f/5$ to name a few. The number of harmonic components that can be identified depends on the accuracy of switching the sampling rate and the background noise. If the governing equations are linear, the pressure response contains contributions with the same oscillation periods and it is a linear superposition of the responses of the individual components. The amplitudes and the phases of the components must be quantified for both the imposing rate signal and the resulting pressure signal. This is readily done using a Fast Fourier Transform (FFT) algorithm (also known as Discrete Fourier Transform), which unravels the periodic signals by recognizing the frequency components. In order to maximize the information provided by harmonic pulse test interpretation, pressure data should be adequately preprocessed adopting detrending methodologies (e.g., Ahn & Horne, 2011; Viberti, 2016) with the aim of separating pure periodic components of the signal from nonperiodic components.

An analytical solution of the diffusivity equation with harmonic boundary conditions incorporating both wellbore storage (C) and skin (S) effects is available in other publications (Fokker et al., 2018; Salina Borello et al., 2017) for the most common scenarios considering early time effects due to the well geometry (partial penetration, horizontal well) or late-time effects (i.e., closed boundary, sealing fault). The derivation for an unbounded aquifer (an aquifer in infinite acting radial flow regime) incorporating wellbore storage, skin effects, and late-time behavior, is presented in Appendix A. The pressure response function for the harmonic component with angular frequency ω is given as

$$R = \frac{p}{\tilde{q}} = \frac{K_0[\xi] + S\xi K_1(\xi)}{k\xi K_1[\xi] + i\omega W_S(K_0[\xi] + \xi S K_1[\xi])} \tag{5}$$

where K_0 and K_1 are modified Bessel functions of the second kind, evaluated for the dimensionless complex argument ξ that contains the imposed frequency and geometric and reservoir parameters:

$$\xi = r_w\sqrt{\frac{i\omega}{\kappa}} \tag{6}$$

and W_S is the scaled wellbore storage:

$$W_S = \frac{\mu C}{2\pi h} \tag{7}$$

For the remaining symbols in this equation see Nomenclature section.

The response function, equation (5), is a complex number. Its absolute value describes the amplitude of the pressure response in relation to rate constraint; its argument describes the phase delay. Positive skin increases amplitude and changes phase of the signal over the full frequency spectrum. Wellbore storage predominantly reduces amplitude at higher frequencies due to the term with ω in the denominator of equation (5).

Equation (5) can be used as a type curve to estimate reservoir properties by minimizing an objective function that penalizes the difference between amplitude ratio and phase difference as determined from the FFT analysis of measurements and as calculated with the model parameters (Fokker et al., 2012). This approach, however, does not guarantee the uniqueness of the matching parameter set, since several combinations of the (k, S) couple might provide very similar results in terms of amplitude ratio. Therefore, a derivative approach analogous to conventional oil field well test analysis but developed in the frequency domain

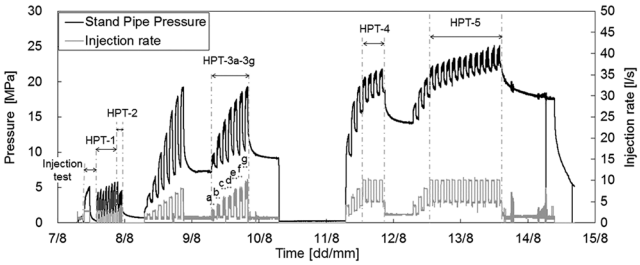

Figure 2. Pohang PX-1 soft stimulation record.

and represented versus the corresponding oscillation period (Fokker et al., 2018; Hollaender, Hammond, & Gringarten, 2002) was adopted to overcome the limitation of the aforementioned.

It should be pointed out that a longer pulse oscillation period T_f allows for a better description of the spectrum at low frequencies, which could significantly improve the interpretation. This is related to the increasing reservoir investigation radius with longer times (Fokker et al., 2018):

$$r_i = 1.5\sqrt{\frac{kT_f}{2\pi\mu c_t\phi}} \tag{8}$$

Moreover, the optimal duration of each semiperiod ($T_f/2$) should be significantly longer than the duration of wellbore storage effects. The shorter the duration of the semiperiod, the more difficult it is to maintain a constant rate and the more challenging it is for the on-site operator to make frequent rate changes at the right time in wells not equipped with automatic remote control.

3. Pohang PX-1 Test Description

The Pohang EGS development in Korea was started in 2010 (Park et al., 2017; Song et al., 2015). Two wells were drilled: the PX-1 and the PX-2 well. The reservoir at the target depth (around 4,300 m) is mainly composed of granodiorite and granitic gneiss (Table 1). Rock mass is highly fractured. Stimulation treatment was first performed on the PX-2 well early in 2016. Stimulation of PX-1 followed in December 2016, and second stimulation on PX-2 in March/April 2017. The present paper focuses on the second stimulation of PX-1, carried out in August 2017 (Hofmann et al., 2019), which is characterized by nine harmonic pulse tests performed on top of background injection rate.

Soft stimulation was applied—it was defined as an injection scheme aimed at minimizing induced seismic events. Our focus, however, is on monitoring the effectiveness of the stimulation treatments. This monitoring was programmed in the form of harmonic pulse tests superimposed on stimulation average rates, preceded by an injection/fall-off test and two harmonic pulse tests with lower injection rates performed to characterize the system before the actual stimulation operations.

Based on well and reservoir knowledge (Hofmann et al., 2019), the input data required for interpretation are summarized in Table 1. Figure 2 presents the full history of injection rates and resulting pressures. The first activity was a straight injection test of which details are reported in Table 2. This was followed by HPT-1, starting 7 August at 14:00. Pulses with a 60-min oscillation period were employed—30-min injection and 30-min shut-in during each oscillation. This test was almost immediately followed by a harmonic pulse test with 6-min pulses (HPT-2). Together, these tests were meant to provide a baseline for the further treatment of the reservoir and associated monitoring. A first fracture opening test was performed on 8 August. This was followed by a second test on 9 August, with a harmonic pulse test of a 6-min oscillation period on top of every increasing injection rate (1 hr each). These short-period monitoring tests are called HPT-3a – HPT-3g. After a long shut-in and flowback on 10 August, the first actual soft stimulation test was performed on 11 August. In principle, the last three oscillations of this treatment could be interpreted as a harmonic pulse test, HPT-4, as those stimulation injection pulses had the same magnitude and duration; oscillation period for this test was 120 min, with alternating high and low injection rates, each lasting 1 hr. However, the number of oscillations was not sufficient to guarantee a reliable signal decomposition in the frequency domain, which synthetic studies have suggested

Table 2
Summary of Injection/Fall-Off Tests in Pohang PX-1

ID	Start time	End time	Flow period duration (hr)	Injection rate (l/s)
Injection	2017-08-07 9:31	2017-08-07 11:30	1.97	2.84
Fall-off	2017-08-07 11:30	2017-08-07 14:00	2.50	0

Table 3
Summary of Harmonic Pulse Tests in Pohang PX-1 Soft Stimulation Treatment.

ID	Start time	End time	Oscillation period (min)	Number of oscillations	Average injection rate (l/s)	Injection rate pulse amplitude (l/s)
HPT-1	2017-08-07 14:00	2017-08-07 22:00	60	8	1.45	1.45
HPT-2	2017-08-07 22:00	2017-08-07 23:00	6	10	1.45	1.45
HPT-3a	2017-08-09 07:00	2017-08-09 08:00	6	10	2.1	0.8
HPT-3b	2017-08-09 09:00	2017-08-09 10:00	6	10	3.0	0.9
HPT-3c	2017-08-09 11:00	2017-08-09 12:00	6	10	3.9	0.9
HPT-3d	2017-08-09 13:00	2017-08-09 14:00	6	10	5.0	1.0
HPT-3e	2017-08-09 15:00	2017-08-09 16:00	6	10	5.9	1.0
HPT-3f	2017-08-09 17:00	2017-08-09 18:00	6	10	7.0	1.0
HPT-3g	2017-08-09 19:00	2017-08-09 20:00	6	10	7.9	1.0
HPT-4	2017-08-11 13:00	2017-08-11 21:00	120	4	7.5	2.5
HPT-5	2017-08-12 14:00	2017-08-13 14:00	120	12	7.5	2.5

should be at least five (Salina Borello et al., 2017). The last train of pulses on 13 and 14 August, with 12 usable oscillation periods of 120 min could also be interpreted as a harmonic pulse test (HPT-5). The operational characteristics of the harmonic pulse tests are summarized in Table 3.

The fluid was injected into the wellbore using one of the two mud pumps of the rig that was on site throughout the operations. The flow rate was controlled manually by an operator who turns a physical knob to increase or decrease the flow rate. Pressure was measured directly at the wellhead (wellhead pressure data, WHP) and at the rig (stand pipe pressure, SPP). SPP was measured every 2–3 s while wellhead pressure was recorded every second with a resolution of 0.1 MPa. Rates were monitored by measuring the number of strokes of the mud pump and acquired with the same sampling.

4. Pohang Test Results

Flow rate and pressure data had to be preprocessed before the application of the FFT algorithm to maximize the information achieved through HPT interpretation. First, SPP data were synchronized and resampled to 1 s, with a stepwise linear approximation, to have the same regular sampling as the rate data; and test sequences of complete oscillations were extracted. No bottom hole pressure data were available; however, SPP data were considered reliable since problems related to phase separation (segregation, etc.) from bottom hole to wellhead conditions were no issue. Wellhead data were not used in the frequency analysis because of the low resolution (0.1 MPa). Then, data were detrended with a heuristic approach suggested by Viberti et al. (2018; see Appendix B for details) to improve the identification and extraction of the signal periodic components as well as to enhance the quality of the results. Finally, a selection of the oscillations to be used is required because a minimum number of regular pulses is necessary to identify the frequencies. Oscillations were not perfectly regular because flow rate variations were imposed manually by an operator. Additionally, unstable flow rates may be observed for values about 2 l/s or lower because the mud pumps are not designed for such low flow rates (~1 l/s is the limit) as for drilling, higher rates are used. Moreover noise was observed on SPP data, especially at high-pressure levels as in HPT-5. Most likely the noise is imputable

Table 4
Summary of Interpretation Results

Test	Permeability thickness (mD m)	Skin (−)	Wellbore storage (m^3/bar)	Investigation radius (m)
Injection/fall-off	84	−3.68	0.005	1,253
HPT-1	84	−3.6	0.005	316
HPT-5 (oscillations 1–6)	350	−3.3	Not detectable from derivative; imposed according to HPT-1 interpretation results	913
HPT-5 (oscillations 7–12)	440	−3.3	Not detectable from derivative; imposed according to HPT-1 interpretation results	1,023

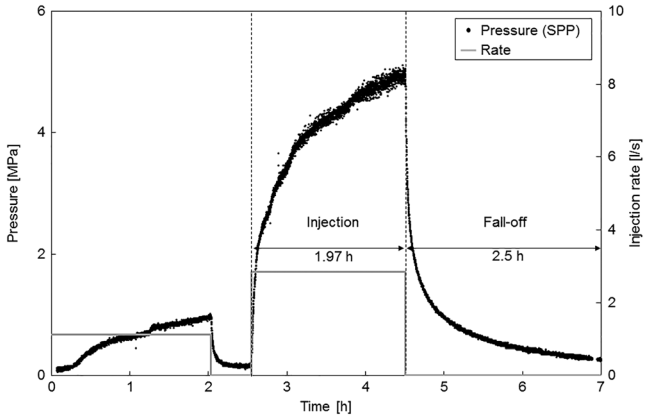

Figure 3. Pohang PX-1 injection/fall-off test.

to the low precision of SPP pressure gauge, which is usually just used to give a rough number of the pressure for drilling operations. Oscillations characterized by irregular duration and rates or very noisy pressure data must be discarded. Selection was made after statistical analysis of durations and rate values of flow periods making up each sequence of pulses.

We deemed interpretation of HPT-2 and HPT-3 unfeasible because of a too short oscillation period (6 min), which corresponded to a small investigation radius and a pressure response of the formation completely masked by wellbore storage. Interpretation of HPT-4 was not completely reliable due to the limited number of complete oscillations available (only 4). Conversely, interpretation of HPT-1 and HPT-5 was successful.

Comparison of injection test with baseline test HPT-1 and test performed during the soft stimulation HPT-5 is summarized in Table 4. An increase in permeability can be seen, probably due to the fracture opening caused by increased pressure, while the skin value is coherent. Interpretation details are given in sections 4.1 and 4.2.

4.1. Baseline Test: Injection 2 and HPT-1

The injection fall-off test was successfully interpreted using conventional type curves. Pressure data were quite clean (Figure 3) and, despite the short fall-off duration (2.5 hr), the horizontal stabilization was clearly visible. From the derivative of the injection period and subsequent fall-off (Figure 4), a clear difference in stabilization is observed, which is due to the difference in temperature between injected fluid (ambient temperature) and reservoir fluid (about 130 °C). The interpretation was performed with a commercial software (Saphir by KAPPA Engineering). Thus, the conventional-type curve analysis was adopted to match pressure variation and pressure derivative curves on the log-log plot ([Figure 5a], measured pressure vs time profile [Figure 5b] and Horner plot [Figure 5c]). The interpretation led to assessing the transmissivity value before the stimulation process (kh = 84 mD m). Negative skin is observed ($S = -3.68$), which is coherent with a well connected to a pattern of natural fractures (Lietard, 1999).

HPT-1 recorded data are reported in Figure 6. The derivative of an injection/fall-off test, an HPT, and even conventional well test can be compared on the same dimensionless log-log plot if proper nondimensional parameters are adopted for pressure variation, time, amplitude ratio, and harmonic period (Fokker et al., 2018):

$$T_{\mathrm{D}=\frac{T}{2\pi}\frac{k}{\mu c_t \phi r_w^2}};\ t_{\mathrm{D}=\Delta t\frac{k}{\mu c_t \phi r_w^2}} \tag{9}$$

$$P_{\mathrm{D}} = R\frac{\pi kh}{B\mu};\ \ p_{\mathrm{D}} = \frac{\Delta p}{\mathrm{q}}\frac{\pi kh}{B\mu} \tag{10}$$

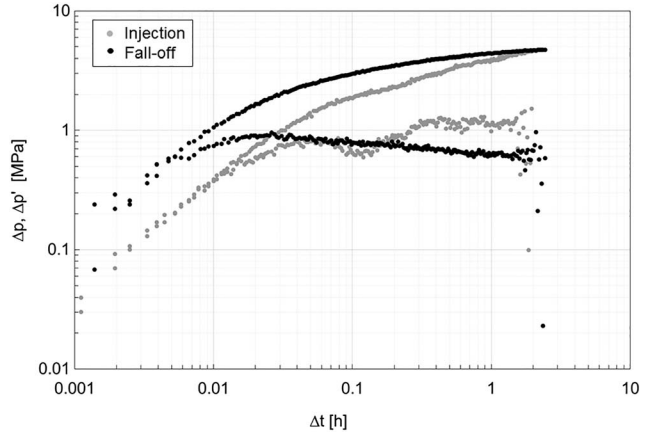

Figure 4. Comparison between injection and fall-off derivatives.

In the presented case history, the derivative of HPT-1 superimposes on the derivative of the fall-off period of the injection/fall-off test in dimensionless terms (Figure 7), thus assuring coherence in wellbore storage, skin, and permeability estimate. Taking into account equation (9) and knowing that the duration of the fall-off is 2.5 times the duration of oscillation period of HPT-1, the derivative of the fall-off covers a dimensionless time interval 5π times greater than the derivative of HPT-1. The corresponding radii of investigation, calculated according to equations (2) and (8), respectively, are reported in Table 4. The results obtained from the interpretation in the frequency domain of HPT-1 are in very good agreement with those provided by the injection test (see Table 4 and Figure 8). Thanks to the quality of the pressure data, affected by limited noise, the derivative in the frequency domain is smooth and allows clear identification of interpretation models especially for early time phenomena. Middle time phenomena can be recognized but are less evident and affected by

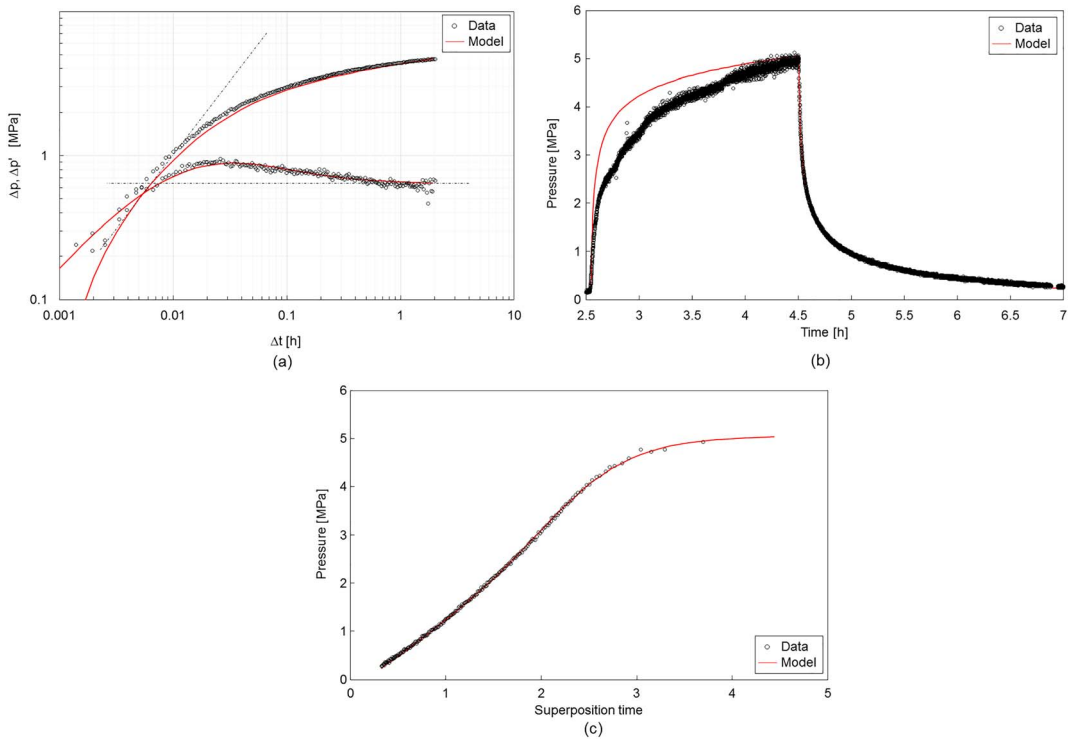

Figure 5. Fall-off test conventional interpretation: (a) log-log plot, (b) history plot, and (c) Horner plot.

uncertainty as a consequence of the short oscillation period. As expected, this does not allow robust identification of the horizontal stabilization and, in turn, of the match point. Three possible matches are shown in Figure 8, characterized by different permeability-thickness product values (kh). The blue and the green matches identify an uncertainty range of kh, which is 70–110 mD m. No acceptable matches were obtained with smaller nor higher values of kh. The uncertainty is thus limited. Moreover, a visual inspection of semilog plot of amplitude ratio versus oscillation period (analogous to Horner plot) and the phase delay plot helps reducing uncertainty by indicating the red match as the more reliable.

It should be noted that phase delay fitting is generally less representative than derivative match, especially for low oscillation period components, which are strongly affected by irregularity in the periodicity. Such components represent the early time effects (i.e., wellbore storage and skin). However, being skin detectable in semilog plot and log-log plot from high oscillation period components, the joint inspection of the three graphs should prevent erroneous interpretations.

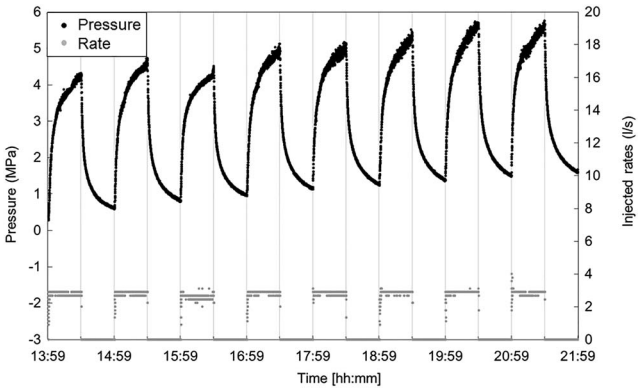

Figure 6. Pohang PX-1 pulse test HPT-1.

4.2. Soft Stimulation Test: HPT-5

The HPT-5 recorded data are reported in Figure 9. The SPP data measured during the entire test are affected by significant levels of noise, increasing with injection rate and pressure, from high (±0.25 MPa) to very high (±1 MPa). WHP were affected by a significantly slighter noise, which was maintained constant during the test; however, the gauge resolution (0.1 Mpa) was too low to allow a derivative analysis. Regardless, comparison with WHP allowed to assess SPP noise that is likely due to the low precision of the gauge; moreover, WHP data showed that the maximum pressure increase observed during each semiperiod of the test would decrease gradually with progressive oscillations (from about 2.5 MPa on the first semiperiod to about 1.5 MPa on the last one), which could be symptomatic of a slight increase in permeability during the stimulation itself. This behavior is present also in the SSP pressure data but is less

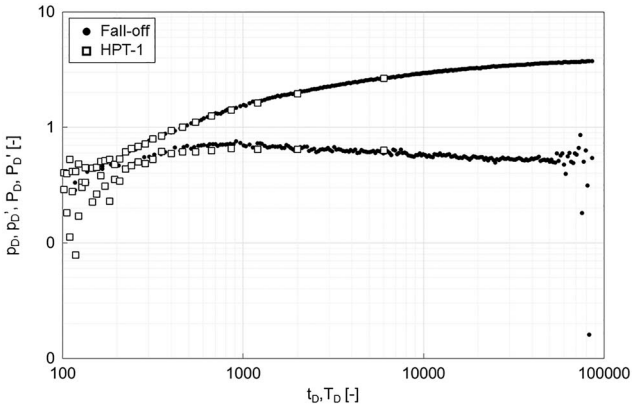

Figure 7. Dimensionless comparison of conventional fall-off derivative and HPT-1 derivative.

clear due to the significant amount of noise. A subdivision of test data into two groups helped to isolate the effect of very high noise to a subset of data as well as to possibly confirm the permeability increase. Therefore, the test was divided into two groups of oscillations: oscillations 1 to 6, less noisy, and oscillations 7 to 12, noisier. Oscillation 13 was discarded due to the anticipated interruption of the second injection semiperiod.

Log-log plot of the derivative of the first six oscillations is shown in black in Figure 10. In this case the early time effects were not detectable because of the background noise on pressure data that affected mainly high frequency components of the signal ($T < 0.1$ hr); thus, $C = 0.005$ m^3/bar was assumed based on HPT-1 interpretation. Conversely, horizontal stabilization corresponding to middle time behavior is clearly detectable, due to the longer oscillation period, thus assuring good interpretation robustness.

Log-log plot of the derivative of the last six oscillations is shown in red in Figure 10. The measured pressure data are affected by a high level of noise that reflects on an amplitude ratio derivative which is quite noisy until $T = 0.39$ hr. The comparison between the derivative of the first and the second group of oscillations confirms around 20% increase in permeability.

Comparison between derivative curves obtained for HPT-1 and for HPT-5 showed higher permeability in the latter test (Figure 11 and Table 4): a fourfold increase was observed. The increase could indicate effectiveness of the stimulation treatment, but this cannot be unequivocally proven. The increase could also be due to temporary opening of fractures during injection as a result of increased injection pressures. Whether stimulation should be considered effective depends on the post-treatment performance for which no information was

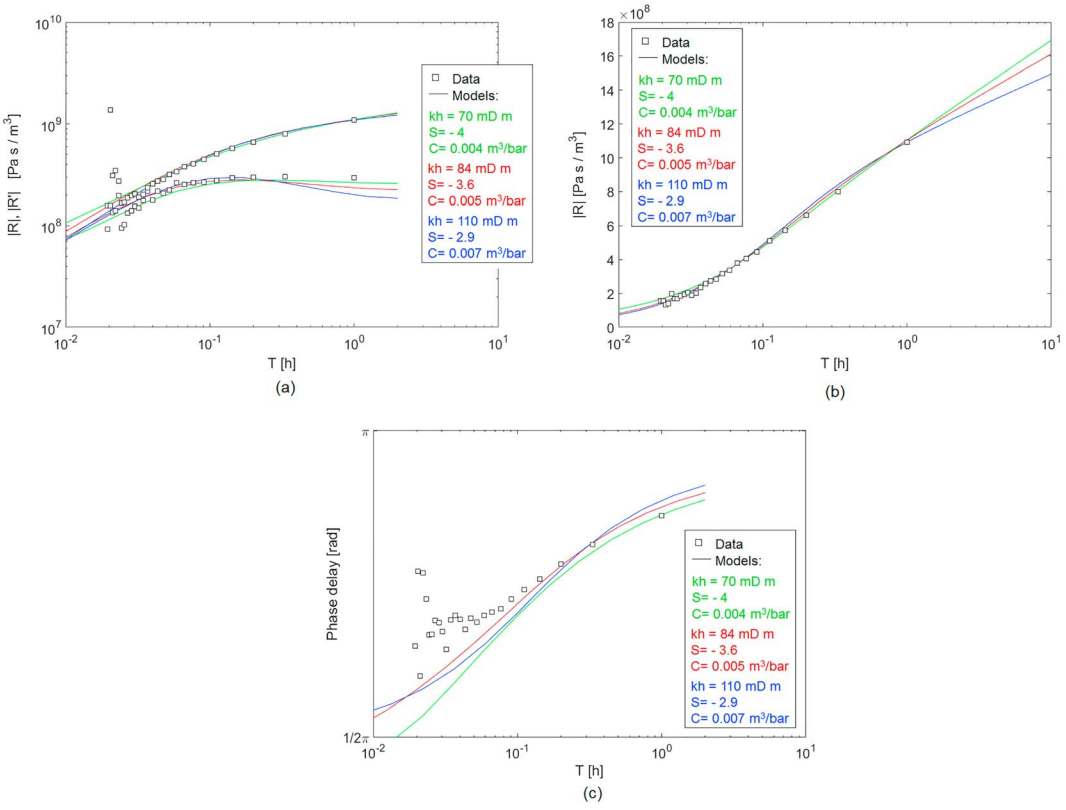

Figure 8. Different possible interpretations in the frequency domain of HPT-1: (a) log-log plot of $|R|$and$|R'|$, (b) semilog plot of$|R|$, and (c) phase delay.

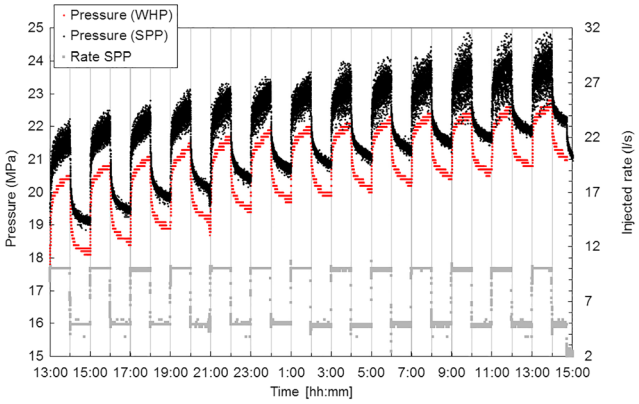

Figure 9. Pohang PX-1 pulse test HPT-5.

available. Injection was stopped, and flow back was initiated after a M_w = 1.9 event triggered the seismic traffic light system.

5. Discussion of the Results

The results provided by the interpretation of the derivative in the frequency domain of the baseline HPT-1 and by the interpretation of the fall-off derivative of the injection test produced consistent results. The interpretation of the HPT conducted during the Soft Stimulation Operations (HPT-5) showed increased permeability values. Compressibility was not varied in the three interpretations. Since the period of oscillation of HPT-5 almost doubled the period of oscillation of HPT-1, the corresponding investigation radiuses are different ($r_{\text{i HPT5}} = \sqrt{2}\, r_{\text{i HPT1}}$), and thus, the kh difference (84 mD m vs 350 mD m) could be explained by a different average permeability of different investigated reservoir zones. However, such a configuration could imply a strong permeability contrast near $r_{\text{i HPT1}}$, detectable as a radial composite on the pressure derivative, which is not the case neither in the fall-off test nor in the HPT-5, both spanning an investigation radius about 1 km (see Table 4). Thus, it is more reasonable to assume that fracture opening caused by increased pressure induced the permeability increase observed during the treatment. Such interpretation is endorsed by the permeability difference observed between interpretation of the first six oscillations of HPT-5 and the last five oscillations, which share the same oscillation period, and thus investigates the same reservoir area. However, the application of a constant value of oscillation period in different HPT conducted at successive times is preferable when permeability monitoring purposes are the aim.

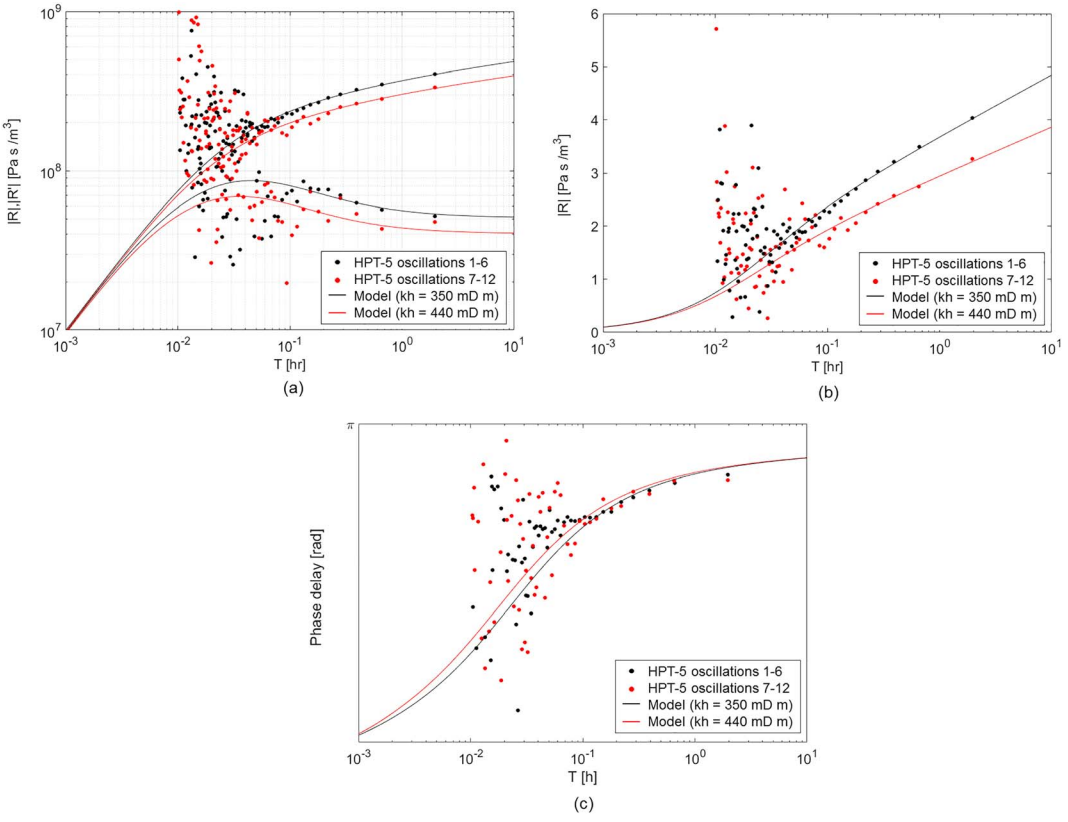

Figure 10. Interpretation in the frequency domain of HPT-5: (a) log-log plot of |*R*|and|*R'*|, (b) semilog plot of|R|, and (c) phase delay.

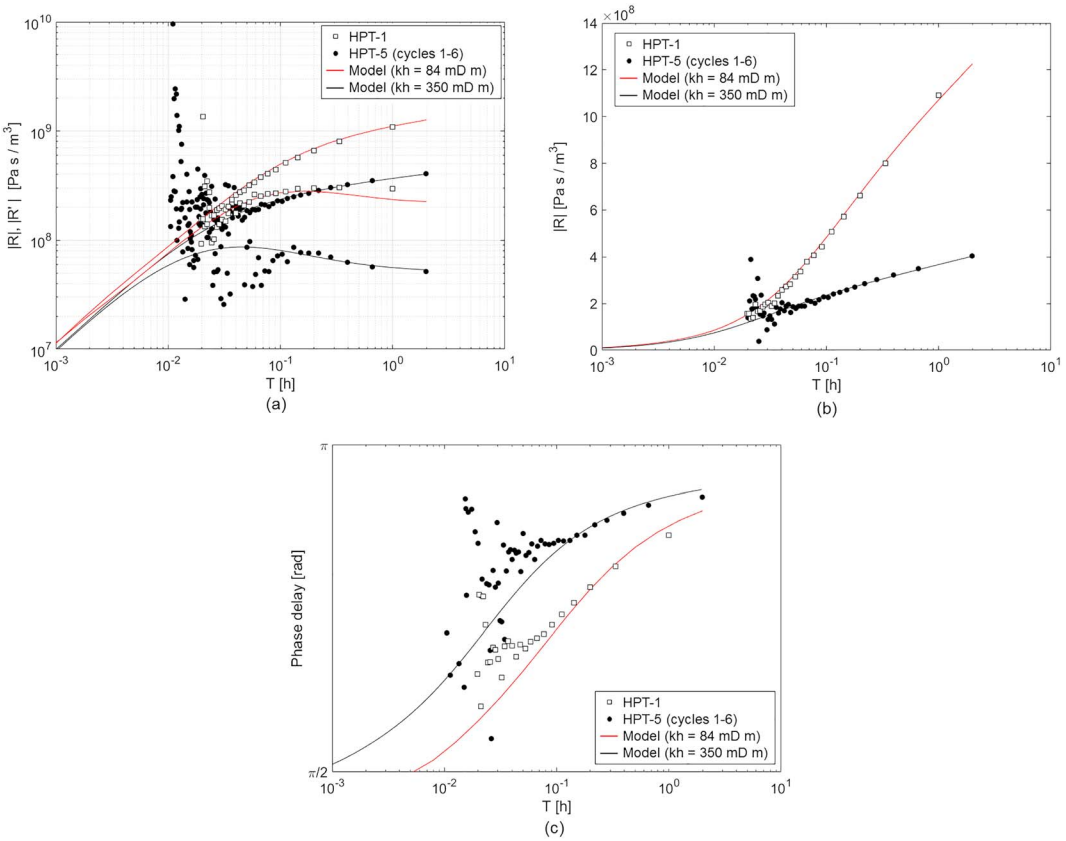

Figure 11. Compared interpretation of HPT-1 and HPT-5: (a) log-log plot of |*R*|and|*R'*|, (b) semilog plot of|R|, and (c) phase delay.

The analysis and interpretation of the HPT data highlighted the importance of a proper selection of oscillation periods in the preliminary test design phase. In fact, oscillation periods of tests HPT-1 and HPT-5, which were 1 and 2 hr, respectively, were enough to assess the horizontal stabilization indicative for the permeability-thickness product. Conversely, the oscillation period of tests HPT-3 was 6-min only, which was not enough to overcome the duration of wellbore storage effect. As a consequence permeability was not detectable from HPT-3 interpretation. HPT design must thus be performed carefully with particular attention to wellbore storage and investigation distance. Short-oscillation-period tests may be adequate only if a downhole shut-in tool were to be employed and a representative investigation distance were reachable. Moreover, the use of the same period of oscillation is recommended for subsequent HPT conducted for permeability monitoring purposes.

Other critical issues potentially compromising the reliability of the proposed pressure data interpretation were the following: (1) low resolution, as for WHP (0.1 MPa), which made derivative curve unfeasible and (2) strong noise, as for SPP pressure in HPT-5, likely due to the low SPP gauge precision. The quality of the derivative of HPT-5 was compromised for the high-frequency components making the characterization of wellbore storage parameter, which is an early time effect, unfeasible.

The signal of a HPT contains two numbers for each frequency tested: the amplitude of the response and the phase. For the determination of the phase the two signals—imposed rates and measured pressures—must be carefully synchronized. An offset immediately results in an error of the phase of especially the smaller oscillation periods (the higher frequencies). Synchronization can be performed manually by identifying corresponding moments of abrupt changes in rate and in pressure.

As already mentioned, during the interpretation process in the frequency domain three diagnostic plots were available: (1) the log-log plot of amplitude ratio and its derivative versus oscillation period, (2) the semilog plot of amplitude ratio versus oscillation period, and (3) the phase delay. Among the three plots, the log-

log plot is the only one that (given a reliable set of data and proper test design) allows the independent characterization of wellbore storage, skin, and kh. As a consequence the role of semilog plot and the phase delay plot is mainly the validation and quality check of interpretation results.

6. Conclusions

We employed an analytical solution in the frequency domain for HPT interpretation represented in terms of a derivative plot. The method provides an interpretation approach for HPT data comparable with conventional well test interpretation (Fokker et al., 2018). The methodology was applied for interpreting data acquired during a sequence of HPT tests on an EGS in Pohang, Korea. A preliminary injection/fall-off test was carried out before the sequence of HPT. Derivative analyses of an injection/fall off test and HPT produced identical curves when the injection test was interpreted in the time domain and the HPT in the frequency domain. The HPT produced the same estimate of hydraulic parameters as the injection test but could be conducted without disturbing stimulation operations. The interpretation of the HPT conducted during the Soft Stimulation Operations showed increased permeability values during the treatment, probably due to the fracture opening caused by increased pressure. The test demonstrated the applicability and the usefulness of HPT for monitoring well operations during injection.

The present test used the PX-1 well both for imposing the rate and for measuring the pressure response. In an interference setup, the pressure response can also be monitored in a different well. The result is the determination of hydraulic properties between the two wells. When an observation well is employed to evaluate hydraulic communication and estimate hydraulic properties between two wells, the total duration of the oscillations sequence must be long enough to allow the signal to travel from the pulsing well to the observation well. The main advantages provided by the proposed methodology with respect to the pulse interference test proposed by Johnson et al. (1966), which allows to interpret the pressure data registered at the observer well only, are the possibility of interpreting the pressure signal generated at the pulsing well, thus maximizing the available information and improving the level of characterization of the formation.

The formation tested was a fractured granite with a clear pressure-dependent permeability. A natural extension of the interpretation would be to incorporate the fracture opening behavior into the analysis method. This would require including an effective reservoir compressibility in the equations and a dependence of permeability on pressure. Geomechanical correlations that assess the effective stresses working on the fractures must then be developed for these tests. In addition, fracture opening correlations versus effective stress and a fracture opening-permeability correlation are required; to this end, we suggest something along the lines of fracture opening models developed by Bandis et al. (1983) and used for shale gas production (Bagheri & Settari, 2008; Shahid et al., 2015, 2016). The geomechanical treatment should follow an approach similar to that of Vinci et al. (2015).

We believe HPT is a valuable tool to complement conventional well testing. It is an ideal monitoring tool since it can be deployed during ongoing operations. Our formulation, in terms of a derivative plot similar to transient well testing interpretation, makes its interpretation straightforward. Permeability-height and wellbore storage can be readily determined from a straight-line analysis in the derivative plot; skin can then be estimated using a curve-fitting algorithm.

Nomenclature

ϕ	porosity, dimensionless
μ	viscosity
ω	angular frequency (=2π/T)
B	formation volume factor
C	wellbore storage
c_t	total compressibility
h	net pay
i	complex unit

k	reservoir permeability
kh	permeability-thickness product
K_0, K_1	modified Bessel functions of the second kind
p	pressure
p_ω	pressure harmonic component
$\|P\|$	amplitude of harmonic components of pressure
P_{D}, P_{D}	dimensionless pressure amplitude and its derivative with respect to lnT
Δp	pressure increment from the beginning of the flow period
$\Delta p'$	derivative of the pressure increase with respect to the logarithm of time increase
q	volumetric rate
$\widetilde{q}$	scaling of volumetric rate, equation (A6)
r_{i}	investigation radius
r_{w}	well radius
R	pressure-rate ratio of harmonic components
$\|R\|$	amplitude of R
$\|R'\|$	amplitude of derivative of R with respect to lnT
S skin	dimensionless
T	oscillation period
t_{D}	dimensionless time
T_{D}	dimensionless oscillation period
T_{f}	fundamental oscillation period
Δt	time increase from the beginning of the flow period
Δt_{fo}	duration of the fall-off
x_{MP}	abscissa of the match point (MP)
y_{MP}	ordinate of the match point (MP)

Appendix A

In a homogeneous aquifer, the flow is described by the diffusivity equation:

$$\phi c \frac{\partial p}{\partial t} = \nabla \left[\frac{k}{\mu} \nabla p \right] \tag{A1}$$

where ϕ is the rock porosity, c is the total compressibility, k is the rock permeability, μ is the water viscosity, p is the pressure, and t is the time.

When a piecemeal homogeneous subsurface is assumed, the diffusivity equation is linear. We obtain

$$\frac{\partial p}{\partial t} = \kappa \nabla^2 p \tag{A2}$$

$$\kappa = \frac{k}{\phi \mu c} \tag{A3}$$

Under the assumption of linearity, the pressure and flow solution of a reservoir with many wells and changing production rates can then be added to the solution of the harmonic test. The pressure response of each frequency component of the imposed rate variation can be recognized via the Fourier transform. There will be no frequency mixing; therefore, each frequency component can be treated independently. The final pressure is then a superposition of the responses to all the frequency components present in the imposed flow rate, added to the background signal.

Considering each frequency independently, we write the pressure solution for each frequency as the product of a space-dependent and a time-dependent function:

$$p(\mathbf{r}, t) = p_\omega(\mathbf{r}) e^{i\omega t} \tag{A4}$$

The angular frequency is defined as $\omega = \frac{2\pi}{T}$, with T the oscillation period of the imposed harmonic signal. This results in a time-independent differential equation for p_ω:

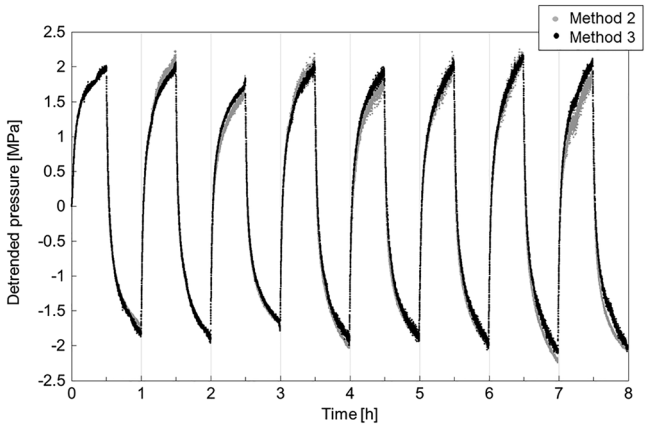

Figure B1. Detrending of HPT-1.

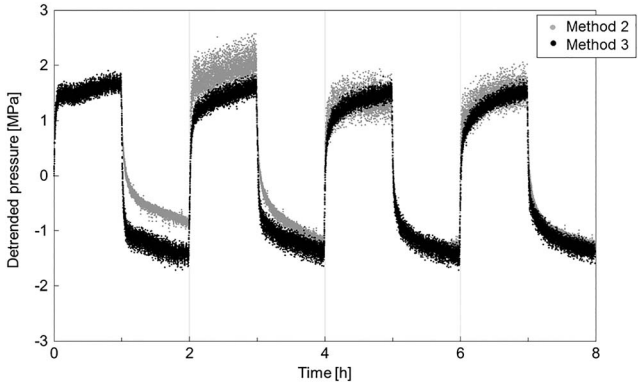

Figure B2. Detrending of HPT-4.

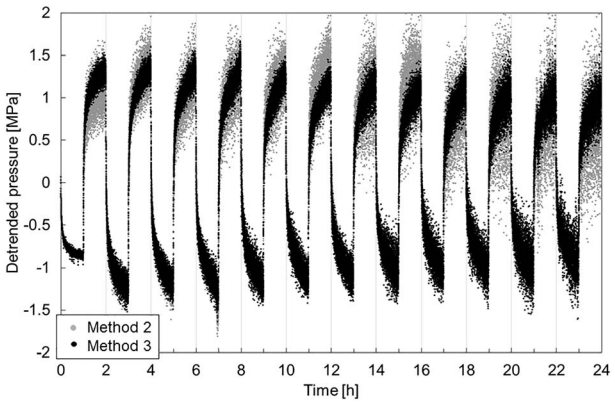

Figure B3. Detrending of HPT-5.

$$i\omega p_\omega(\mathbf{r}) = \kappa \nabla^2 p_\omega(\mathbf{r}) \tag{A5}$$

For the scaling of the volumetric rates q we take

$$\frac{\mu q}{2\pi h} = \widetilde{q} = \widetilde{q}_\omega e^{i\omega t} \tag{A6}$$

In the adopted nomenclature, the thickness of the contributing reservoir layers is indicated by h and the rate is assumed positive for injection.

For an infinite reservoir with radial symmetry the diffusivity equation can be rewritten into radial coordinates. The first boundary condition for each component then is a harmonic signal on the flow rate corrected for the wellbore storage effect. The second boundary condition is a zero pressure at large distances from the well, as the net flow of the harmonic signal is zero. We obtain

$$i\omega p_\omega(r) = \kappa \frac{1}{r}\frac{\partial}{\partial r}\left(r\frac{\partial p_\omega}{\partial r}\right) \tag{A7}$$

$$k\left[r\frac{\partial p}{\partial r}\right]_{r=r_w} = -\widetilde{q} + W_S \frac{\partial}{\partial t}\left([p(r,t)]_{r=r_w} + \Delta p_S\right) \tag{A8}$$

$$[p(r,t)]_{r\to\infty} = 0 \tag{A9}$$

$$W_S = \frac{\mu C}{2\pi h} \tag{A10}$$

where r is the radial distance from the tested well, h is the producing-layer thickness, and C is the wellbore storage coefficient. The term Δp_S has been added to p since the wellbore storage must be calculated using the wellbore pressure, that is, the pressure at $r = r_w$ corrected for the additional pressure drop due to the skin.

The additional pressure drop due to skin S is (Dake, 1978):

$$\Delta p_S = \frac{q\mu}{2\pi k h} S \tag{A11}$$

Recalling Darcy's law, $q = -\frac{2\pi r k h}{\mu}\frac{\partial p}{\partial r}$, the additional pressure drop due to skin can be expressed as

$$\Delta p_S = -S\left[r\frac{\partial p}{\partial r}\right]_{r=r_w} = -S\left[r\frac{\partial p_\omega}{\partial r}\right]_{r=r_w} e^{i\omega t} \tag{A12}$$

and the boundary condition for the differential equation becomes independent of time as well:

$$i\omega p_\omega(r) = \kappa \frac{1}{r}\frac{\partial}{\partial r}\left\{r\frac{\partial p_\omega}{\partial r}\right\} \tag{A13}$$

$$(k + i\omega W_S S)\left[r\frac{\partial p_\omega}{\partial r}\right]_{r=r_w} = -\widetilde{q}_\omega + i\omega W_S p_\omega(r_w) \tag{A14}$$

$$[p(r,t)]_{r\to\infty} = 0 \tag{A15}$$

The solution to these equations is the zeroth-order modified Bessel function of the second kind, K_0:

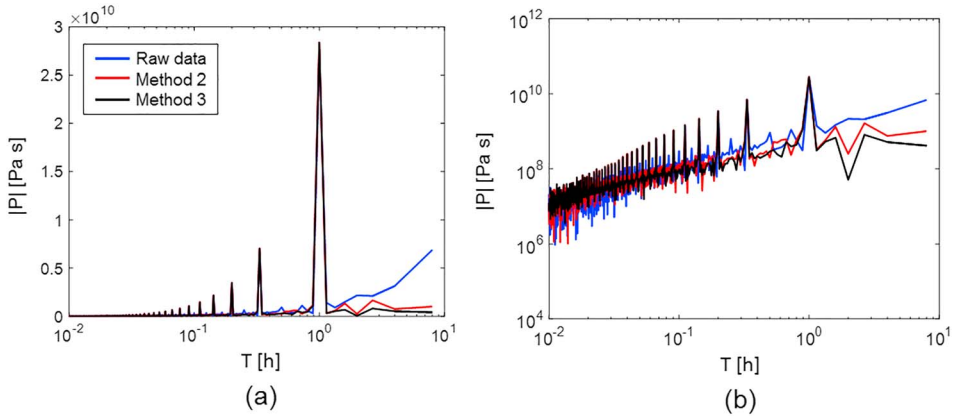

Figure B4. Pressure spectrum of HPT-1 before and after detrending: (a) linear scale and (b) log scale.

$$p_\omega(r) = \frac{\tilde{q}_\omega K_0\left[\xi \frac{r}{r_w}\right]}{k\xi K_1[\xi] + i\omega W_S(K_0[\xi] + \xi S K_1[\xi])} \tag{A16}$$

$$\xi = r_w\sqrt{\frac{i\omega}{\kappa}} \tag{A17}$$

The scaling of the function follows from the well boundary condition.

The skin pressure drop is calculated as

$$\Delta p_S = -S\left[r\frac{\partial p_\omega}{\partial r}\right]_{r=r_w} e^{i\omega t} = S\frac{\xi K_1(\xi)}{K_0(\xi)} p_\omega(r) e^{i\omega t} \tag{A18}$$

The pressure components at the wellhead can now be calculated, and we obtain the following response function:

$$R = \frac{p_{\text{well}}(t)}{\tilde{q}} = \frac{1}{\tilde{q}_\omega e^{i\omega t}}[p(r_w t) + \Delta p_S] = \frac{K_0[\xi] + S\xi K_1(\xi)}{k\xi K_1[\xi] + i\omega W_S(K_0[\xi] + \xi S K_1[\xi])} \tag{A19}$$

The multiplier of the oscillatory function is a complex number. Its absolute value describes the amplitude of the pressure response to the rate constraint; its argument describes the phase delay of the response.

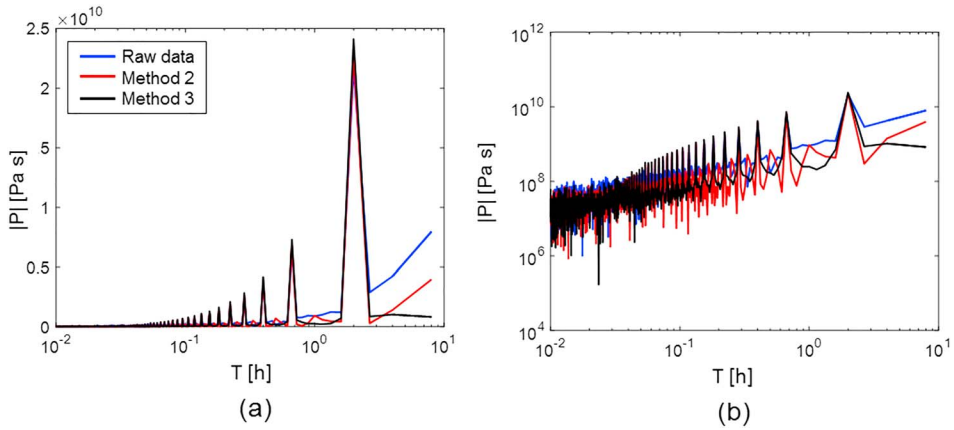

Figure B5. Pressure spectrum of HPT-4 before and after detrending: (a) linear scale and (b) log scale.

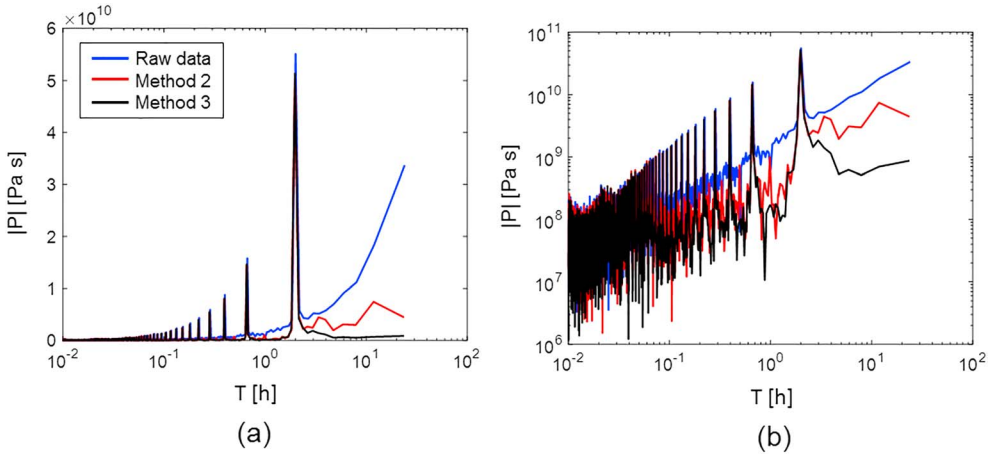

Figure B6. Pressure spectrum of HPT-5 before and after detrending: (a) linear scale and (b) log scale.

Appendix B: Preprocessing by Data Detrending

As part of data preprocessing, pressure data of the harmonic pulse test sequences HPT-1, HPT-4, HPT-5 were detrended (Figures B1, B2, B3) to isolate the periodic component, which is object of the Fourier analysis. Two heuristic approaches presented by Viberti et al. (2018) as Methods 2 and 3 were adopted. In brief Method 2 calculates the reconstructed pressure signal corresponding to a constant rate equal to the maximum oscillation rate for a time vector containing the elements $t_n = \frac{1}{2}T, T, \frac{3}{2}T, 2T, ...n_T T$,and linear wise interpolation is adopted for points in each interval, while Method 3 gives a full heuristic reconstruction of the constant rate pressure signal for all the time samples based on the identification of recurring events. Details are available in Viberti et al. (2018).

Method 3 gave better results improving the signal to noise ratio of pressure spectrum more significantly in all the cases (Figures B4, B5, B6). This happened in first place because noisy pressure data could negatively affect detrending effectiveness of Method 2, but not Method 3 as it is observed marginally in HPT-1 (Figure B1) and to a greater degree in HPT-4 (Figure B2). In second place, Method 3 is able to filter out part of the noise, thus improving data quality of HPT-4 and HPT-5 (Figures B2 and B3, respectively).

Acknowledgments

The research presented in this paper is part of DESTRESS, a project that received funding from the European Union's Horizon 2020 Research and Innovation Program under grant agreement 691728. This work was also supported by the New and Renewable Energy Technology Development Program of the Korea Institute of Energy Technology Evaluation and Planning (KETEP) through a grant (20123010110010) funded by the Korean Government's Ministry of Trade, Industry, and Energy and by the Korea-EU Joint Research Support Program of the National Research Foundation of Korea (NRF) through a grant (NRF-2015K1A3A7A03074226) funded by the Korean Government's Ministry of Science and ICT. Data are available either as supporting information of Hofmann et al., 2019 or upon request (hannes.hofmann@gfz-potsdam.de).

References

Ahn, S., & Horne (2011). The use of attenuation and phase shift to estimate permeability distributions from pulse tests. In *Proceedings - SPE Annual Technical Conference and Exhibition*, 3:2092–2106. Denver, CO. https://doi.org/10.2118/146636-MS.

Ahn, S., & Horne, R.N. (2010). Estimating permeability distributions from pressure pulse testing. In *Proceedings - SPE Annual Technical Conference and Exhibition*, 3:2388–2403. Florence. https://doi.org/10.2118/134391-MS.

Azzarone, E., Beretta, E., Guglielmelli, A., Nunzi, P., & Mariotti, P. (2011). Gas injection testing & PLT—Offshore Eni Experience. In *OMC-2011-064*. OMC: Offshore Mediterranean Conference.

Bagheri, M. A., & Settari, A. (2008). Modeling of geomechanics in naturally fractured reservoirs. *SPE Reservoir Evaluation & Engineering*, *11*(01), 108–118. https://doi.org/10.2118/93083-PA

Bandis, S. C., Lumsden, A. C., & Barton, N. R. (1983). Fundamentals of rock joint deformation. *International Journal of Rock Mechanics and Mining Science and Geomechanics Abstracts*, *20*(6), 249–268. https://doi.org/10.1016/0148-9062(83)90595-8

Banerjee, R., Thompson, L. G., & Reynolds, A. C. (1998). Injection/falloff testing in heterogeneous reservoirs. *SPE Reservoir Evaluation & Engineering*, *1*(06), 519–527. https://doi.org/10.2118/52670-PA

Barreto, A. B., Peres, A. M., & Pires, A. P. (2011). Water injectivity tests on multilayered oil reservoirs. In *Brasil Offshore*. Macaé, Brazil: Society of Petroleum Engineers. SPE142746. https://doi.org/10.2118/142746-MS

Beretta, E., Tiani, A., Lo Presti, G., & Verga, F. (2007). Value of injection testing as an alternative to conventional well testing: Field experience in a sour-oil reservoir. *SPE Reservoir Evaluation and Engineering*, *10*(02), 112–121. https://doi.org/10.2118/100283-PA

Black, J. H., & Kipp, K. L. J. (1981). Determination of hydrogeological parameters using sinusoidal pressure tests: A theoretical appraisal. *Water Resources Research*, *17*(3), 686–692. https://doi.org/10.1029/WR017i003p00686

Boughrara, A. A., Peres, A. M., Chen, S., Machado, A. A. V., & Reynolds, A. C. (2007). Approximate analytical solutions for the pressure response at a water-injection well. *SPE Journal*, *12*(01), 19–34. https://doi.org/10.2118/90079-PA

Bourdet, D. (2002). *Well west analysis: The Use of Advanced Interpretation Models: Handbook of Petroleum Exploration and Production, 3*. Amsterdam: Elsevier Science B.V. ISBN: 978-0-444-54988-4.

Bourdet, D., Whittle, T. M., Douglas, A. A., & Pirard, Y. M. (1983). New set of type curves simplifies well test analysis. *World Oil*, *196*(6), 95–106.

Cardiff, M., Bakhos, T., Kitanidis, P. K., & Barrash, W. (2013). Aquifer heterogeneity characterization with oscillatory pumping: Sensitivity analysis and imaging potential. *Water Resources Research*, *49*, 5395–5410. https://doi.org/10.1002/wrcr.20356

Cardiff, M., & Barrash, W. (2015). Analytical and semi-analytical tools for the design of oscillatory pumping tests. *Groundwater*, *53*(6), 896–907. https://doi.org/10.1111/gwat.12308

Chen, Y., & Renner, J. (2018). Exploratory use of periodic pumping tests for hydraulic characterization of faults. *Geophysical Journal International*, *212*(1), 543–565. https://doi.org/10.1093/gji/ggx390

Copty, N. K., & Findikakis, A. N. (2004). Stochastic analysis of pumping test drawdown data in heterogeneous geologic formations [Analyse stochastique des données de rabattement obtenues en pompages d'essai dans des formations géologiques hétérogènes]. *Journal of Hydraulic Research*, *42*(sup1), 59–67. https://doi.org/10.1080/00221680409500048

Dake, L. P. (1978). *Fundamentals of reservoir engineering*. Amsterdam: Elsevier Scientific Pub. Co. 978-0-444-41830-2

Despax, D., Dovis, R., Fedele, J.-M., & Martin, J.-P. (2004). Method and device for determining the quality of an oil well reserve. *U.S. Patent*, *6*, 801–857.

El-Khazindar, Y., Ramzi Darwish, M., & Tengirsek, A. (2002). Environmentally friendly well testing. In *SPE International Conference on Health, Safety and Environment in Oil and Gas Exploration and Production*. Kuala Lumpur: Malaysia. Society of Petroleum Engineers. 74106MS. https://doi.org/10.2118/74106-MS

Fokker, P. A., Renner, J., & Verga, F. (2013). Numerical modeling of periodic pumping tests in wells penetrating a heterogeneous aquifer. *American Journal of Environmental Sciences*, *9*(1), 1–13. https://doi.org/10.3844/ajessp.2013.1.13

Fokker, P. A., Salina Borello, E., Serazio, C., & Verga, F. (2012). Estimating reservoir heterogeneities from pulse testing. *Journal of Petroleum Science and Engineering*, *86-87*, 15–26. https://doi.org/10.1016/j.petrol.2012.03.017

Fokker, P. A., Salina Borello, E., Verga, F., & Viberti, D. (2018). Harmonic pulse testing for well performance monitoring. *Journal of Petroleum Science and Engineering*, *162*, 446–459. https://doi.org/10.1016/j.petrol.2017.12.053

Fokker, P. A., & Verga, F. (2011). Application of harmonic pulse testing to water-oil displacement. *Journal of Petroleum Science and Engineering*, *79*(3–4), 125–134. https://doi.org/10.1016/j.petrol.2011.09.004

Gringarten, A. C., Bourdet, D. P., Landel, P. A., & Kniazeff, V. J. (1979). A comparison between different skin and wellbore storage type-curves for early-time transient analysis. In *SPE Annual Technical Conference and Exhibition*. Las Vegas, Nevada: Society of Petroleum Engineers. SPE8205MS. https://doi.org/10.2118/8205-MS

Guiltinan, E., & Becker, M. W. (2015). Measuring well hydraulic connectivity in fractured bedrock using periodic slug tests. *Journal of Hydrology*, *521*, 100–107. https://doi.org/10.1016/j.jhydrol.2014.11.066.

Habte, A. D., & Onur, M. (2014). Laplace-Transform finite-difference and quasistationary solution method for water-injection/falloff tests. *SPE Journal*, *19*(03), 398–409. https://doi.org/10.2118/168221-PA

Hofmann, H., Zimmermann, G., Farkas, M., Huenges, E., Zang, A., Leonhardt, M., et al. (2019). First field application of the cyclic soft stimulation concept at the Pohang Enhanced Geothermal System Site in Korea. *Geophysical Journal International*, *217*(2), 926–949. https://doi.org/10.1093/gji/ggz058

Hollaender, F., Filas, J. G., Bennett, C. O., & Gringarten, A. C. (2002). Use of downhole production/reinjection for zero-emission well testing: Challenges and rewards. In *Proceedings - SPE Annual Technical Conference and Exhibition* (pp. 2443–2452). San Antonio, TX: Society of Petroleum Engineers (SPE). https://doi.org/10.2118/77620-MS

Hollaender, F., Hammond, P. S., & Gringarten, A. C. (2002). Harmonic testing for continuous well and reservoir monitoring. In *Proceedings - SPE Annual Technical Conference and Exhibition*, (pp. 3071–3082). San Antonio, TX: Society of Petroleum Engineers (SPE). https://doi.org/10.2118/77692-MS

Horner, D. R. (1951). Pressure Build-Up in Wells. Proceedings of the 3rd World Petroleum Congress, 28 May-6 June, TheHague, the Netherlands. pp. 503–521.

Johnson, R. A., Greenkorn, C. R., & Woods, E. G. (1966). Pulse testing: A new method for describing reservoir flow properties between wells. *Journal of Petroleum Technology*, *18*(12), 1599–1604. https://doi.org/10.2118/1517-PA

Kuo, C. H. (1972). Determination of reservoir properties from sinusoidal and multirate flow tests in one or more wells. *Society of Petroleum Engineers Journal*, *12*(06), 499–507. https://doi.org/10.2118/3632-PA

Lee, W. J. (1982). *Well testing*. Dallas, Texas: Textbook Series, SPE.

Levitan, M. M. (2003). Application of water injection/falloff tests for reservoir appraisal: New analytical solution method for two-phase variable rate problems. *SPE Journal*, *8*(04), 341–349. https://doi.org/10.2118/87332-PA

Lietard, O. (1999). Permeabilities and skins in naturally fractured reservoirs: An overview and an update for wells at any deviation. In *Proceedings - SPE European Formation Damage Conference*, 31 May-1 June, Hague, Netherlands. https://doi.org/10.2118/54725-MS

Morozov, P. E. (2013). Harmonic testing of hydraulically fractured wells. *Proceeding of 17th European Symposium on Improved Oil Recovery*. St. Petersburg, Russia, 16-18 April 2013.

Park, S., Xie, L., Kim, K.-I., Kwon, S., Min, K.-B., Choi, J., et al. (2017). First hydraulic stimulation in fractured geothermal reservoir in Pohang PX-2 Well. *Procedia Engineering*, *191*, 829–837. https://doi.org/10.1016/j.proeng.2017.05.250

Renner, J., & Messar, M. (2006). Periodic pumping tests. *Geophysical Journal International*, *167*(1), 479–493. https://doi.org/10.1111/j.1365-246X.2006.02984.x

Rocca, V., & Viberti, D. (2013). Environmental sustainability of oil industry. *American Journal of Environmental Sciences*, *9*(3), 210–217. https://doi.org/10.3844/ajessp.2013.210.217

Rochon, J., Jaffrezic, V., De La Combe, J.L.B., Azari, M., Roy, S., Dorffer, D., et al. (2008). Method and application of cyclic well testing with production logging. In *Proceedings - SPE Annual Technical Conference and Exhibition*, 4:2376–90. Denver, CO. https://doi.org/10.2118/115820-MS.

Rosa, A. J., & Horne, R. N. (1997). Reservoir description by well-test analysis by use of cyclic flow-rate variation. *SPE Formation Evaluation*, *12*(04), 247–254. https://doi.org/10.2118/22698-PA

Salina Borello, E., Fokker, P. A., Viberti, D., Espinoza, R., & Verga, F. (2017). Harmonic-pulse testing for non-Darcy-effects identification. *SPE Reservoir Evaluation and Engineering*, *20*(02), 486–501. https://doi.org/10.2118/183649-PA.S

Shahid, A. S. A., Fokker, P. A., & Rocca, V. (2016). A review of numerical simulation strategies for hydraulic fracturing, natural fracture reactivation and induced microseismicity prediction. *The Open Petroleum Engineering Journal*, *9*(1), 72–91. https://doi.org/10.2174/1874834101609010072

Shahid, A. S. A., Wassing, B. B., Fokker, P. A., & Verga, F. (2015). Natural-fracture reactivation in shale gas reservoir and resulting microseismicity. *Journal of Canadian Petroleum Technology*, *54*(06), 450–459. https://doi.org/10.2118/178437-PA

Song, Y., Lee, T.J., Jeon, J., & Yoon, W.S. (2015). Background and progress of the Korean EGS pilot project, *World Geothermal Congress*, Melbourne, Australia, 19-25 April, Paper No. 01008.

Sun, A. Y., Lu, J., & Hovorka, S. (2015). A harmonic pulse testing method for leakage Detection in deep subsurface storage formations. *Water Resources Research*, *51*, 4263–4281. https://doi.org/10.1002/2014WR016567

Tripaldi, G., Beretta, E., Bertolini, C., Gorlani, A., Costa, A., Latioui, S., et al. (2009). Injection testing: An innovative field application in Berkine basin, Algeria. In *OMC-2009-046*. OMC: Offshore Mediterranean Conference.

Verga, F., & Rocca, V. (2010). Green methodologies to test hydrocarbon reservoirs. *American Journal of Environmental Sciences*, *6*(1), 1–10. https://doi.org/10.3844/ajessp.2010.1.10

Verga, F., & Salina Borello, E. (2016). Unconventional well testing: A brief overview. *Geoingegneria Ambientale e Mineraria*, *149*(3), 45–54.

Verga, F., Viberti, D., & Salina Borello, E. (2008). A new 3-D numerical model to effectively simulate injection tests. In *70th European Association of Geoscientists and Engineers Conference and Exhibition 2008: Leveraging Technology. Incorporating SPE EUROPEC 2008* (Vol. 2, pp. 946–959). Rome: Society of petroleum engineers. https://doi.org/10.2118/113832-MS

Verga, F., Viberti, D., Salina Borello, E., & Serazio, C. (2014). An effective criterion to prevent injection test numerical simulation from spurious oscillations. *Oil & Gas Science and Technology – Revue d'IFP Energies Nouvelles*, *69*(4), 633–651. https://doi.org/10.2516/ogst/2013137

Verga, F., Viberti, D., & Salina Borello, E. (2011). A new insight for reliable interpretation and design of injection tests. *Journal of Petroleum Science and Engineering*, *78*(1), 166–177. https://doi.org/10.1016/j.petrol.2011.05.002

Verga, F., Viberti, D., & Serazio, C. (2012). Estimation of skin components for a partially completed damaged well from injection tests. *Journal of Petroleum Science and Engineering*, *90-91*, 165–174. https://doi.org/10.1016/j.petrol.2012.04.024

Viberti, D. (2016). Effective detrending methodology for harmonic transient pressure response. *Geoingegneria Ambientale e Mineraria*, *149*(3), 55–62.

Viberti, D., Salina Borello, E., & Verga, F. (2018). Pressure detrending in harmonic pulse test interpretation: When, why and how. *Energies*, *11*(6), 1540 MDPI. https://doi.org/10.3390/en11061540

Vinci, C., Steeb, H., & Renner, J. (2015). The imprint of hydro-mechanics of fractures in periodic pumping tests. *Geophysical Journal International*, *202*(3), 1613–1626. https://doi.org/10.1093/gji/ggv247

Woie, R., Hegre, T. M., Gravem, T., & Berger, P. E. (2000). Downhole production testing, a cost effective, safe and environmentally friendly well test method. In *SPE International Conference on Health, Safety and Environment in Oil and Gas Exploration and Production*. Stavanger, Norway: Society of Petroleum Engineers. SPE61183MS. https://doi.org/10.2118/61183-MS